

Adsorption Kinetics and Structural Arrangements of Cetylpyridinium Bromide at the Silica–Aqueous Interface

R. Atkin,[†] V. S. J. Craig,[‡] and S. Biggs^{*,†}

Centre for Multiphase Processes, Department of Chemistry, The University of Newcastle, Callaghan, New South Wales 2308, Australia, and Department of Applied Mathematics, Research School of Physical Sciences, Australian National University, Canberra, Australian Capital Territory 0200, Australia

Received October 2, 2000. In Final Form: March 28, 2001

The adsorption of cetylpyridinium bromide to the silica–aqueous interface has been studied using optical reflectometry and atomic force microscopy (AFM). The effects of pH, electrolyte, and surface preparation on the surface excess and adsorption kinetics are reported. AFM imaging above the critical surface aggregation concentration (CSAC) elucidates spherical surface structures in the absence of electrolyte and elongated cylindrical structures with added electrolyte. At concentrations around the CSAC, adsorption proceeds slowly in the absence of salt and takes hours to reach an equilibrium value. At all other concentrations and even at the CSAC when electrolyte is present, the adsorption is complete within minutes. The concentration range for which slow adsorption is apparent has been termed the slow adsorption region (SAR) of the adsorption isotherm. AFM imaging of surfactant adsorption in the SAR suggests that the slow adsorption kinetics are due to the gradual formation of surface structures in this region. The effects of pH and added electrolyte on surface excess and adsorption kinetics have also been studied. At moderate to high surfactant concentration with added electrolyte, pH increases have little effect on surface excess. In the absence of electrolyte, the surface excess increases with pH as expected, but it is suggested that these increases are primarily due to increased solution ionic strength and not due to increased charge on the substrate. At low surfactant concentrations, added cations compete effectively with the cationic surfactant for adsorption sites, resulting in no detectable adsorption until a pH of ~ 8 is reached.

Introduction

The adsorption of surfactants to the solid–liquid interface is critical for many processes including detergency, wetting, and mineral flotation. To completely quantify the adsorption process, the equilibrium surface excess, the rate of adsorption, and the conformation of the adsorbed layer must be determined. Here, we report measurements on the cetylpyridinium bromide (CPBr)–silica system aimed at elucidating the adsorption process and the structure of adsorbed surfactants. For ionic surfactants at very low concentrations, adsorption occurs via electrostatic interactions between the surface and the monomer, leading to neutralization of the surface charge. As the silica surface has a low charge density, individual charged sites have little influence on the chemistry of neighboring sites. Increasing the bulk surfactant concentration initially has little effect until a well-defined increase in adsorption takes place. The concentration at which this occurs is the hemimicelle concentration (HMC).¹ It is a result of lateral interactions between adsorbed monomers leading to structures or aggregates on the substrate, with headgroups adsorbed to the silica surface.² At this concentration, the surface charge is reversed due to the positive charge associated with the adsorbed aggregates. Further increases in bulk concentration have little influence on the surface excess until the critical surface aggregation concentration (CSAC) is reached. Depending on the system under investigation, the CSAC is typically between one-third and two-thirds of the solution critical micelle concentration (CMC). At the CSAC, the surface excess increases sharply as admicelles

are formed. The term admicelle is used here to describe adsorbed monomer aggregates with headgroups facing both toward the surface and into the solution; incomplete bilayers and surface-adsorbed micelles are included in this definition.²

An inability to reveal the precise structure of the admicelles has made it difficult to quantify the exact mechanism of surfactant adsorption. Atomic force microscopy (AFM) has been used to probe the structure of the adsorbed surfactant layer, but for surfaces that do not template the surfactant structure, these studies have been successful only above the CSAC.³ Spherical admicelles of myristyltrimethylammonium bromide (MTAB) and cetyltrimethylammonium bromide (CTAB) have been observed on silica at a concentration of $2 \times$ the CMC.⁴ Velegol et al. reported a change in adsorbed aggregate structure from spherical to wormlike upon the addition of electrolyte,⁵ while Wanless and Ducker⁶ reported that the addition of electrolyte leads to closer packing of the admicelles on the silica surface. Adsorbed layer structures have also been suggested from neutron reflectivity studies.⁷ However, neutron reflectivity studies are model dependent; therefore, the conclusions are not unequivocal. It should be noted that recent improvements in radiation sources plus the combination of X-ray and neutron scattering experiments are allowing a greater differentiation between structural models.⁸ Until recently, direct measurements

(3) Manne, S.; Gaub, H. E. *Science* **1995**, *270*, 1480–1482.

(4) Liu, J.; Ducker, W. A. *J. Phys. Chem. B* **1999**, *103*, 8558.

(5) Velegol, S. B.; Fleming, B. D.; Biggs, S. R.; Wanless, E. J.; Tilton, R. D. *Langmuir* **2000**, *16*, 2548.

(6) Wanless, E. J.; Ducker, W. A. *J. Phys. Chem.* **1996**, *100*, 3207.

(7) Rennie, A. R.; Lee, E. M.; Simister, E. A.; Thomas, R. K. *Langmuir* **1990**, *6*, 1031.

(8) *Supramolecular Structure in Confined Geometries*; Manne, S., Warr, G., Eds.; ACS Symposium Series 736; American Chemical Society: Washington DC, 1999.

[†] The University of Newcastle.

[‡] Australian National University.

(1) Gaudin, A. M.; Fuerstenau D. W. *Trans. AIME* **1955**, *202*, 958.

(2) Yeskie, M. A.; Harwell, J. H. *J. Phys. Chem.* **1988**, *92*, 2346.

of the adsorption kinetics of surfactants have received little attention. This is primarily due to the difficulty associated with following the fast adsorption of surfactants. The development of ellipsometric methods with high temporal resolution has overcome this barrier.^{5,9–12} These methods give information on the adsorbed layer that is an average of the region over which the observation is made, whereas AFM can probe the length scales of the aggregates in three dimensions. Lateral dimensions (x and y) are investigated using surface images, and information on the surfactant structure in the z dimension is obtained by operating the AFM in force mode.

CPBr and its chloride analogue (CPCI) have been the subject of several adsorption studies.^{13–18} Harrop¹⁸ found that the adsorption of CPBr was highly dependent on pH, with physisorption predominating at low pH values and chemisorption increasing with pH. Gao et al. studied the effect of inorganic salts, alcohols, and urea on the adsorption of CPBr to silica and found that all isotherms exhibited two plateau regions with or without various additives.¹⁷ The subsequent study by Huang et al. on CTAB adsorption¹⁹ revealed a four-region isotherm with the HMC being $\sim 0.5 \times$ the CMC. The regions suggested were a low-surface excess region, a first plateau region beginning at the HMC, a hydrophobic interaction region, and a second plateau. The abrupt increase in adsorption at the HMC was thought to be due to hydrophobic interactions between adsorbed monomers. The effect of pH adjustment on CTAB adsorption was also studied. It was found that, with increasing pH, adsorption was enhanced significantly at low concentrations with the first adsorption plateau either decreased or eliminated, leading to a three-region isotherm. The effect of the addition of electrolyte on surfactant adsorption was also investigated, and it was shown that at low surfactant concentrations adsorption is reduced, the first plateau is significantly shorter, the hydrophobic interactions are enhanced, and the saturation surface excess is increased. The adsorption of CPBr to silica was investigated using flotation measurements by Schwarz et al.,¹⁶ who postulated a tentative adsorption model based on the formation of bilayers and tetralayers. Favoriti et al.¹³ investigated the influence of counterions on the adsorption of cetylpyridinium-based surfactants and found that the binding of aromatic anions to adsorbed aggregates resulted in a 6-fold increase in the plateau surface excess, due to close packing of monomers when associated with the aromatic species.¹³

In a previous study of the adsorption of CTAB to silica,²⁰ we reported that adsorption proceeded slowly at concentrations close to the CSAC. Here, we use the pyridinium analogue, CPBr, to further study this effect. Furthermore, we correlate the data from surface excess measurements with AFM data to elucidate the structural arrangements of the adsorbed surfactants. CPBr absorbs ultraviolet light,

permitting bulk surfactant concentrations to be determined accurately, with a precision of 10^{-7} M, using absorption spectroscopy. This has enabled changes in adsorption behavior, as a result of very small changes in surfactant concentration, to be investigated. We report the role of added electrolyte on the surfactant surface excess and adsorption rate, as determined by optical reflectometry. Additionally, the surface excess and adsorption rate as a function of pH, with and without added electrolyte, are studied in the current work.

Materials and Methods

Silicon wafers were baked at 1000 °C for 100 min in an oxygen atmosphere to produce an oxide layer (SiO₂). Surfaces with lower hydroxyl group density are obtained upon baking due to condensation reactions at the silica surface that result in the formation of siloxane bonds.²¹ The remaining hydroxyl groups are isolated and therefore less likely to participate in hydrogen-bonded stabilization of hydronium ions at the surface.²¹ In solution, these hydroxyl groups are therefore more acidic, and the silica surface will be more highly charged. When used in this state, we call the silica pyrogenic. Pyrogenic silica will slowly rehydroxylate when immersed in water, resulting in what is termed hydroxylated silica. Hydroxylated silica was prepared here by soaking pyrogenic silica in water for 48 h, followed by treating with 10 wt % NaOH for 30 s and rinsing in water and in ethanol before being dried under a nitrogen stream. The thickness of the oxide layer present on the silicon wafer was determined ellipsometrically using an Auto EL-II automatic ellipsometer (Rudolf Research) to be 165 ± 1 nm for both the hydroxylated and the pyrogenic silicas. The refractive indices of silica and silicon used in the determination of surface excess were 3.8 and 1.46, respectively. These wafers were used as the substrates for both reflectometry and AFM adsorption studies.

The optical reflectometry technique used to measure surface excess concentrations follows that described by Dijt et al.²² and has been described in detail in a previous paper.²⁰ Briefly, reflectometry relies upon the changes in the reflective properties of a substrate upon adsorption. In a typical reflectometry experiment, the cell initially contains pure water, and a stable baseline is recorded. Surfactant is then passed into the cell via a two-way valve, and the change in the ratio of the s and p polarizations of the reflected laser beam is recorded, which is proportional to the surface excess. The reflectometer is entirely contained in an incubator, allowing the temperature to be accurately maintained at 25 ± 0.1 °C.

AFM images of adsorbed surfactant structures were obtained using a Nanoscope III AFM (Digital Instruments) operating in the "soft contact" mode as described previously.^{23,24} Silicon nitride cantilevers from Olympus were used. These had sharpened tips with a radius of less than 20 nm and a spring constant of ~ 0.09 N m⁻¹. The images presented in the current study are deflection images, using scan rates of 10 Hz with integral and proportional gains between one and three. AFM experiments were conducted by first passing Milli-Q water into the cell and analyzing the surface for cleanliness. This was ascertained both by analysis of force curves and from images of the substrate. Surfactant solutions were then introduced to the cell, and images of the surface were taken after elapsed times of between 5 min and 24 h. The AFM is also contained in an incubator, allowing the temperature to be accurately maintained at 25 ± 0.1 °C.

KOH (analytical grade), CPBr {1-hexadecylpyridinium bromide, CAS Registry No. 140-72-7} (purity greater than 99%), and KBr (analytical grade) were obtained from Aldrich. The CPBr was recrystallized 2 \times from acetone and freeze-dried. KOH and KBr were oven baked for 24 h at 600 °C to remove organic contaminants. All water used was filtered, distilled, and passed

(9) Tiberg, F.; Jonsson, B.; Lindman, B. *Langmuir* **1994**, *10*, 3714.

(10) Eskilsson, K.; Yaminsky, V. V. *Langmuir* **1998**, *14*, 2444.

(11) Dijt, J. C.; Cohen-Stuart, M. A.; Fleer, G. J. *Adv. Colloid Interface Sci.* **1994**, *50*, 79.

(12) Furst, E. M.; Pagac, E. S.; Tilton, R. D. *Ind. Eng. Chem. Res.* **1996**, *35*, 1566.

(13) Favoriti, P.; Mannebach, M. H.; Treiner, C. *Langmuir* **1996**, *12*, 4961.

(14) Bury, R.; Favoriti, P.; Treiner, C. *Colloids Surf., A* **1998**, *139*, 99.

(15) Favoriti, P.; Treiner, C. *Langmuir* **1998**, *14*, 4961.

(16) Schwarz, R.; Heckman, K.; Strnad, J. *J. Colloid Interface Sci.* **1988**, *124*, 50.

(17) Gao, Y.; Du, J.; Gu, T. *J. Chem. Soc., Faraday Trans. 1* **1987**, *83*, 2671.

(18) Harrop, R. J. *Surf. Technol.* **1978**, *7*, 81.

(19) Huang, Z.; Ma, J.; Gu, T. *Acta Chim. Sin.* **1989**, *2*, 105.

(20) Atkin, R.; Craig, V. S. J.; Biggs, S. *Langmuir* **2000**, *16*, 9374.

(21) Iler, R. K. *The Chemistry of Silica*; Wiley-Interscience Publishers: New York, 1979.

(22) Dijt, J. C.; Cohen-Stuart, M. A.; Fleer, G. J. *Adv. Colloid Interface Sci.* **1994**, *50*, 79.

(23) Manne, S.; Cleveland, J. P.; Gaub, H. E.; Stucky, G. D.; Hansma, P. K. *Langmuir* **1994**, *10*, 4409.

(24) Fleming, B. D.; Wanless, E. J. *Microsc. Microanal.* **2000**, *6*, 104.

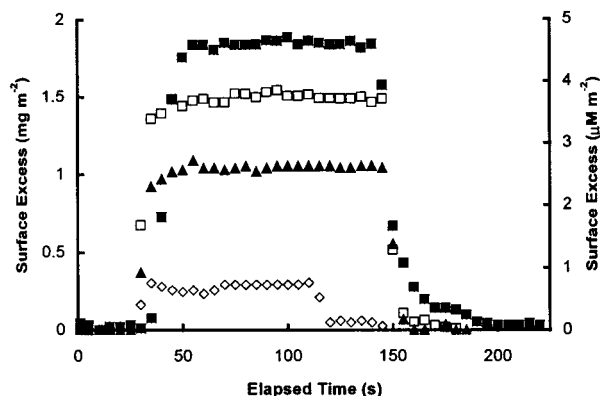


Figure 1. Measured surface excess of CPBr at the pyrogenic silica–solution interface vs time with no added electrolyte for CPBr concentrations of 0.3 (open diamonds), 0.6 (filled triangles), 0.7 (open squares), and 1.0 (filled squares) mM. The CPBr solution is first passed into the cell at ~ 40 s, leading to surfactant adsorption. The plateau level of adsorption is maintained while the CPBr solution is flowing into the cell. The surface excess rapidly returns to zero when water is reintroduced to the cell.

through a Millipore filtration unit before use. The solution CPBr concentration was quantified precisely spectrophotometrically at 258 nm.

Results

The adsorption of CPBr onto pyrogenic silica as a function of time for a range of concentrations was investigated. The measured surface excess as a function of time is presented in Figure 1. Initially, the reflectometry cell contains only water, permitting a stable baseline to be recorded. In this case, the CPBr solution is introduced at ~ 40 s, resulting in a sharp increase in surface excess. Within a further 20 s, the equilibrium surface excess is reached, the magnitude of which is dependent upon the solution surfactant concentration. Note that for any system where the equilibrium surface excess is rapidly attained, no changes in surface excess are observed after the plateau is reached. In these examples, water was passed into the cell after ~ 100 s. The desorption of the CPBr from the surface results, and the surface excess rapidly returns to zero. These data are typical for any system where rapid equilibrium is achieved, regardless of the pH or electrolyte concentration. We term the concentration over which this occurs the rapid adsorption region (RAR). By performing a series of these experiments for a range of surfactant concentrations, an adsorption isotherm can be determined.

Adsorption isotherms for CPBr on pyrogenic and hydroxylated silica and CPBr with 10 mM KBr on pyrogenic silica are presented in Figure 2. The adsorption isotherm for CPBr in the absence of added electrolyte displays a low level of surface coverage at concentrations up to 0.1 mM, with the surface excess below 0.15 mg m^{-2} . This level of coverage is usually associated with charge neutralization of the silica surface. For CTAB, neutralization of the surface charge on an equivalent silica surface has been reported at $5.5 \times 10^{-5} \text{ mM}$,²⁵ and this corresponds to a surface excess of approximately 0.15 mg m^{-2} . Above 0.1 mM, the surface excess of CPBr increases with concentration until saturation levels of surface coverage are obtained at ~ 0.6 mM. This is in agreement with Gao et al., who determined an isotherm with essentially the same features.¹⁷ The region of increasing surfactant

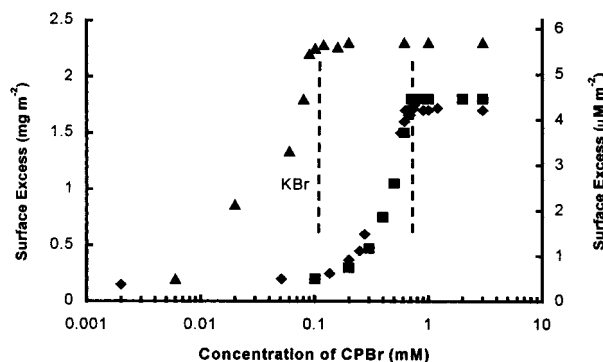


Figure 2. Measured surface excess vs CPBr concentration in the presence of 0.01 M KBr on pyrogenic silica (triangles) and in the absence of 0.01 M KBr on pyrogenic (squares) and hydroxylated (diamonds) silica. The dotted lines indicate the CMC for each system.

adsorption between 0.3 and 0.6 mM in the absence of electrolyte is of particular interest in this study and is addressed in detail below. The rapid increase in surface excess is due to the formation of aggregates on the surface at the CSAC. The saturation surface excess of CPBr for pyrogenic silica and hydroxylated silica was found to be 1.7 and 1.6 mg m^{-2} , respectively. A similar difference in saturation surface excess was observed previously for CTAB using pyrogenic and hydroxylated silica.²⁰ The addition of electrolyte (10 mM KBr) increases the surface excess over the range of surfactant concentrations studied and results in the maximum surface excess being reached at a lower concentration. The CSAC for CPBr with 10 mM KBr on pyrogenic silica is estimated to be 0.08 mM, and the maximum surface excess is 2.3 mg m^{-2} .

Further information concerning surfactant adsorption at the solid–liquid interface can be obtained using direct in situ AFM. Images of the pyrogenic silica–solution interface immersed in an aqueous solution of 2.75 mM CPBr are presented in Figure 3. This concentration is above both the CSAC and the CMC. Figure 3a was obtained without added electrolyte, and Figure 3b was obtained with 0.01 M KBr. In the absence of electrolyte, adsorbed spherical structures are observed on the silica surface with an adsorbed layer thickness of $2.0 \pm 0.2 \text{ nm}$ and an average peak to peak distance of $13.3 \pm 0.5 \text{ nm}$. The layer thickness was determined from deflection by the “push-through” distance described by Wanless and Ducker.⁶ This relies upon the surface and the tip experiencing an electrostatic repulsion until, at a specific separation, the tip pushes through the adsorbed layer and makes adhesive contact with the substrate. The peak to peak distance reports the average spacing between the peaks of adsorbed aggregates. The adsorption density was found to be 80 ± 5 aggregates per $10\,000 \text{ nm}^2$. In the presence of 10 mM KBr, most of the structures observed appear elongated. Peak to peak distances in this case were $8.1 \pm 0.2 \text{ nm}$, and the thickness of the adsorbed layer was found to be $3.4 \pm 0.5 \text{ nm}$. This sphere to cylinder transition has been observed previously for CTAB, adsorbed both at the silica surface⁵ and in bulk solution at higher electrolyte concentrations.²⁶ No discernible change in structure could be seen in the images collected regularly over 6 h. Similarly, no change in the force vs distance profiles was observed.

In a previous study of the adsorption of CTAB to silica,²⁰ a slow increase in surface excess was reported in the region

(25) Neivandt, D. J.; Gee, M. L.; Tripp, C. P.; Hair, M. L. *Langmuir* **1997**, *13*, 2519.

(26) Magid, L. J.; Han, Z.; Warr, G. G.; Cassidy, M. A.; Butler, P. D.; Hamilton, W. A. *J. Phys. Chem. B* **1997**, *101*, 7919.

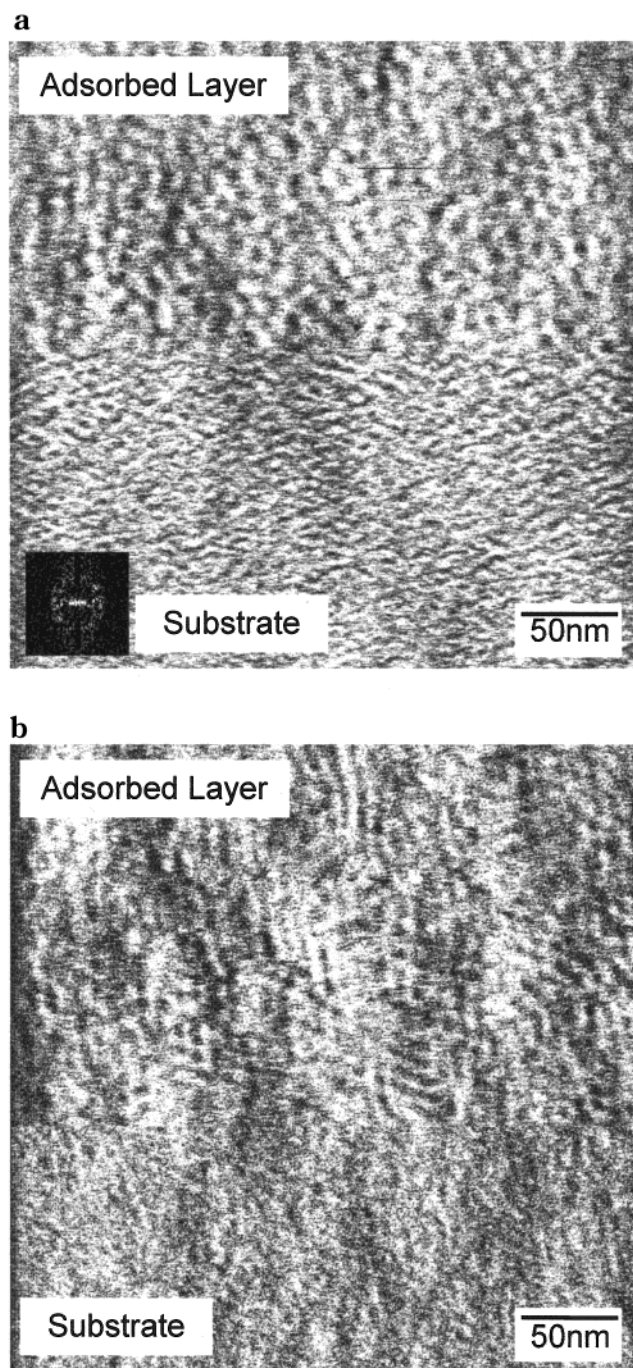


Figure 3. (a) AFM image obtained of the silica–solution interface immersed in an aqueous solution of 2.75 mM CPBr, revealing adsorbed aggregates with approximately circular profiles in the upper portion of the image. The slow scan direction is down the page. The underlying silica surface is imaged in the lower portion of the page when a higher imaging force is applied. The Fourier transform shown at the bottom left of the image indicates a common separation distance but no orientational ordering. (b) AFM image obtained of the silica–solution interface immersed in an aqueous solution of 2.75 mM CPBr with 0.01 M KBr, indicating elongated or “wormlike” aggregates. The slow scan direction is down the page. The underlying silica surface is imaged in the lower portion of the page when a higher imaging force is applied.

of the CSAC. In the current investigation, this phenomenon is studied more thoroughly by investigating the change in surface excess due to small changes in solution surfactant concentration around the CSAC for CPBr on hydroxylated silica. The surface excess as a function of

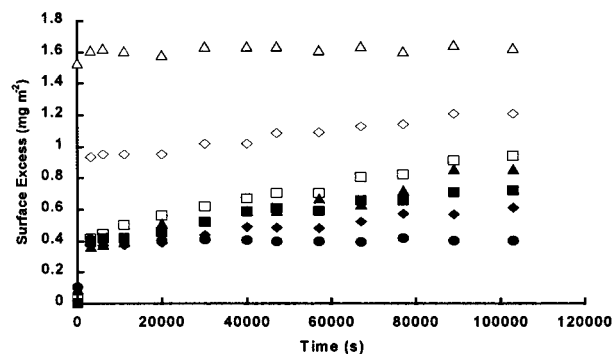


Figure 4. Measured surface excess of CPBr at the hydroxylated silica–solution interface vs time for CPBr concentrations of 0.202 (filled circles), 0.274 (filled diamonds), 0.284 (filled triangles), 0.306 (filled squares), 0.315 (open squares), 0.336 (open diamonds), and 0.554 (open triangles) mM with no added electrolyte. Adsorption occurs over a much greater time period than for other concentrations. The surface excess initially increases rapidly to 0.4 mg m^{-2} and then continues to increase over many hours.

time for a series of concentrations is presented in Figure 4. A concentration increase from 0.202 to 0.554 mM CPBr leads to a corresponding change in surface excess of $0.4\text{--}1.6 \text{ mg m}^{-2}$. The latter is the saturation level of surface excess. In both cases, adsorption occurs rapidly, indicating the lower and upper boundaries of the concentrations over which adsorption precedes slowly (hours). We call the concentration region bounded by these two results the slow adsorption region (SAR). Adsorption experiments were conducted using several CPBr solutions spanning the SAR. For each case up to a concentration of 0.315 mM, the surface excess initially rises rapidly to around 0.4 mg m^{-2} , which is the level attained with 0.2 mM CPBr. However, the surface excess then increases further with time, albeit at a much slower rate.

Discussion

Surface Excess and Surface Structure. Adsorption isotherms for cationic surfactants adsorbed to silica substrates have been studied extensively.^{5,27,28} In contrast to CTAB, which has the same hydrocarbon chain length, there is no intermediate plateau exhibited in the CPBr adsorption isotherm; hence, the equilibrium adsorption isotherm is of the single-step variety. The absence of a stepwise increase in adsorption is likely to be due to the effective decreased headgroup area of CPBr relative to CTAB, resulting in greater association between adsorbed surfactant monomers. This would allow surface aggregation to occur more readily. However, without a definitive knowledge of the adsorbed aggregate structures below the CSAC, it is not possible to make inferences concerning the interactions that produce a single- or double-step isotherm. The maximum adsorption density of approximately 1.7 mg m^{-2} is typical of results for CPBr on silica in the absence of added electrolyte, with literature values^{17,18} ranging from 1.6 to 1.8 mg m^{-2} .

The chemistry of the silica surface is known to vary depending on the method of preparation. As our silicon wafers are of high purity, the surfaces are uncomplicated by the presence of metal ions. The adsorption of CPBr onto pyrogenic and hydroxylated silica was investigated in this study. The isotherm for CPBr on these two types

(27) Fuerstenau, D. W.; Wakamatsu, T. *Faraday Discuss. Chem. Soc.* **1975**, *59*, 157.

(28) Somasundaran, P.; Fuerstenau, D. W. *J. Phys. Chem.* **1966**, *70*, 90.

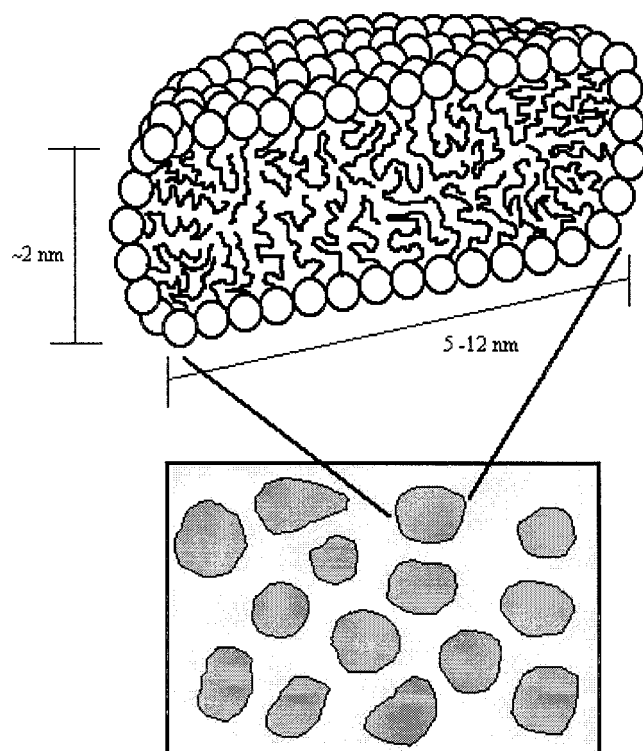


Figure 5. Schematic of the average admicelle structure determined from AFM and reflectometry studies of 2.75 mM CPBr adsorbed at the hydroxylated silica–solution interface. The admicelles or lucano typically are 2 nm thick, have a radius of 4.3 nm, and contain ~ 350 monomers. The counterions associated with the admicelle are not represented in this schematic. Approximately 45% of the silica surface is covered by lucano, and the remaining surface bears very little adsorbed surfactant.

of silica is compared in Figure 2. The surface excesses at low concentrations are similar, but the saturation surface excess is higher for pyrogenic silica. Corresponding results have been noted in a previous study for the adsorption of CTAB.²⁰

The AFM images of CPBr adsorbed to the silica surface in the absence of electrolyte (Figure 3a) suggest that the density of aggregate adsorption is approximately 80 admicelles per $10\,000\text{ nm}^2$. The admicelles are clearly not uniform in size or shape. However, if we take an average admicelle to have a spherical profile of radius 4.3 nm (from the AFM image), a thickness of 2.0 nm (from the force measurement), and a density of 950 kg m^{-3} (from extrapolating the density data for liquid bromoalkanes and adjusting for some loss of bromine due to ionization), the calculated adsorption excess obtained is 1.8 mg m^{-2} . This is in agreement with the adsorption excess obtained using reflectometry. Thus, the structure of the adsorbed layer is that of flattened and enlarged micelles, somewhat like Lucano Italian bread, separated by regions with very low levels of adsorbed surfactant. The surface is intermediate between a patchy bilayer and adsorbed spherical micelles. Each “lucano” has on average ~ 350 monomers, and approximately 50% of the surface is covered. The proposed structure of a typical admicelle, seen in Figure 3a, is shown schematically in Figure 5. Upon addition of electrolyte, the headgroup area decreases. Therefore, the structure of the admicelles must change to encompass the corresponding decrease in interfacial curvature and the increase in surface excess. This is achieved by elongation of the admicelle to form wormlike structures.

The plateau surface excess for CPBr was found to increase with the addition of 10 mM KBr to 2.3 mg m^{-2} . Additionally, the CSAC was found to decrease to approximately 0.08 mM. These results may be explained by the screening of the headgroup charge of the surfactant by the electrolyte. Addition of electrolyte reduces the headgroup area. This allows aggregation to proceed at lower concentrations, resulting in the lowering of the solution CMC and the CSAC. An additional important consequence of the reduction in headgroup area is the associated increase in the critical packing parameter (cpp).²⁹ Aggregates with lower curvature are formed when the cpp is increased. This is manifested in an increase in surface excess (cf. Figure 2) and a change in aggregate structure from spheres to cylinders (cf. Figure 3). Details of the structure of the cylinders can be inferred from the peak to peak distance and layer thickness determined using AFM. Wanless and Ducker⁶ have shown that increasing the ionic strength of the bulk solution allows adsorbed surfactant aggregates to pack closer together on the surface. However, in the current study, it was found that the peak to peak distance (the spacing between the wormlike surfactant aggregates) was essentially unchanged when electrolyte was added. In order for the peak to peak distances to be maintained in the presence of electrolyte while the surface excess has increased, the width of the aggregates themselves must be increasing and the regions between the aggregates consequently decreasing. Additionally, the thickness in the z direction of the wormlike aggregates is slightly less than that of the spherical aggregates determined in the absence of electrolyte, which indicates some flattening of the structures.

Slow Adsorption Region. We now examine the SAR previously observed with CTAB.²⁰ The current study has revealed that CPBr also exhibits a SAR, which we have studied in more detail. As shown in Figure 4, solution CPBr concentrations of 0.2 and 0.55 mM are sufficient to lead to a plateau coverage of 0.4 and 1.6 mg m^{-2} , respectively. It is within these two boundaries, and only between these boundaries, that long-term increases in CPBr adsorption were noted. Beyond this region, adsorption reaches an equilibrium rapidly, characteristic of the RAR.

At CPBr concentrations between 0.274 and 0.306 mM, the surface excess rapidly increases to approximately 0.4 mg m^{-2} but then continues to increase at a greatly reduced rate. Changes in solution CPBr concentrations of only 0.01 mM are sufficient to bring about notable increases in the rate of the secondary adsorption. The rate of this secondary increase in adsorption is proportional to the surfactant concentration, as shown in Figure 6. Additionally, an increase in the solution surfactant concentration to 0.336 mM CPBr leads to a fast increase in the level of surface coverage to 0.9 mg m^{-2} , followed by a similar slow increase in the levels of adsorption. The rate of the secondary adsorption in this case is decreased over that observed for concentrations between 0.274 and 0.306 mM. Adsorption results obtained for other CPBr concentrations between 0.33 and 0.55 mM displayed the same features as 0.336 mM. Importantly, the magnitude of the initial increase was seen to increase with concentration. The data between 0.33 and 0.55 mM are not shown here for reasons of clarity. The result for 0.336 mM CPBr is obviously of a different form to those between 0.274 and 0.306 mM. At 0.336 mM, the slight increase in concentration leads to greater hydrophobic interactions between adsorbed mono-

(29) Israelachvili, J. N. *Intermolecular and Surface Forces*, 2nd ed.; Academic Press: New York, 1995.

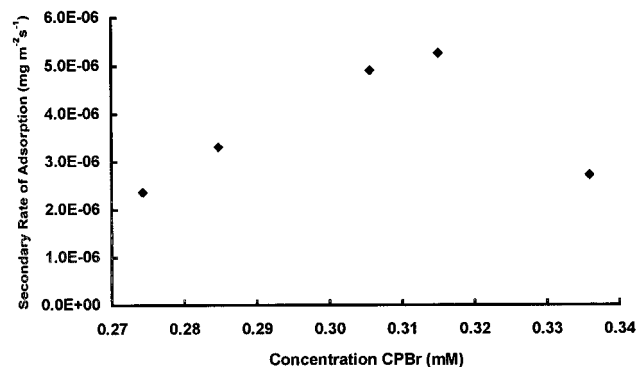


Figure 6. Rate of secondary adsorption of CPBr to the silica–solution interface. The secondary rate of adsorption is calculated from the measured surface excess between 100 (after the rapid initial increase had been attained) and 103 000 s. Note that the rate of the secondary increase is proportional to the bulk solution concentration up to a CPBr concentration of 0.315 mM. When the CPBr concentration is increased to 0.335 mM, the rate of secondary adsorption is reduced. At this concentration, the primary adsorbed amount is much greater at 0.9 mg m^{-2} (see Figure 4).

mers, which results in the rapid formation of admicelles. This could be analogous to the step in the CTAB adsorption isotherm,²⁰ which occurs at the structural transition between hemimicelles and admicelles. In the case of CPBr, the step occurs over a very narrow concentration range so that it is essentially unnoticed. For each of these experiments, it appears that the surface excess has not reached plateau levels after 30 h. Limitations associated with data collection prevented longer observation times.

These results suggest that in the secondary phase of the adsorption process adsorbing surfactants are filling surface adsorption sites stochastically. As the concentration is increased, the probability of a monomer adsorbing is also increased, leading to a faster rate of secondary adsorption. The initial level of surface excess is higher for 0.336 mM (0.9 mg m^{-2}), which suggests that the adsorbed surfactant layer is more complete in the initial stages of adsorption than that obtained with slightly lower bulk concentrations. Consequently, there is a reduced number of adsorption sites available on the surface, which leads to the observed reduced secondary rate of adsorption at this concentration.

AFM imaging was used to investigate the structural changes that must accompany these slow increases in adsorption. AFM images of the silica surface at 20 min and 22.5 h after the injection of 0.3 mM CPBr are presented in Figure 7. After 20 min elapsed, there was no evidence of any structure present in the adsorbed layer on the silica surface, despite a surface coverage of $\sim 0.4 \text{ mg m}^{-2}$ obtained by reflectometry. However, after 22.5 h, the presence of an adsorbed layer structure is clear, though perhaps not as well-defined as at higher concentrations (Figure 3a). An adsorption density of approximately 0.7 mg m^{-2} is obtained by reflectometry at this concentration.

Further evidence of a change in the layer structure over many hours can be found in measurements of force vs separation. Figure 8 shows that initially for the substrate in water we have virtually no repulsion and a small attraction, consistent with an attractive van der Waals force. At a pH of 5.5, the silica surface is expected to carry a negative surface charge. The silicon nitride cantilever tip is close to its isoelectric point³⁰ and is therefore nearly

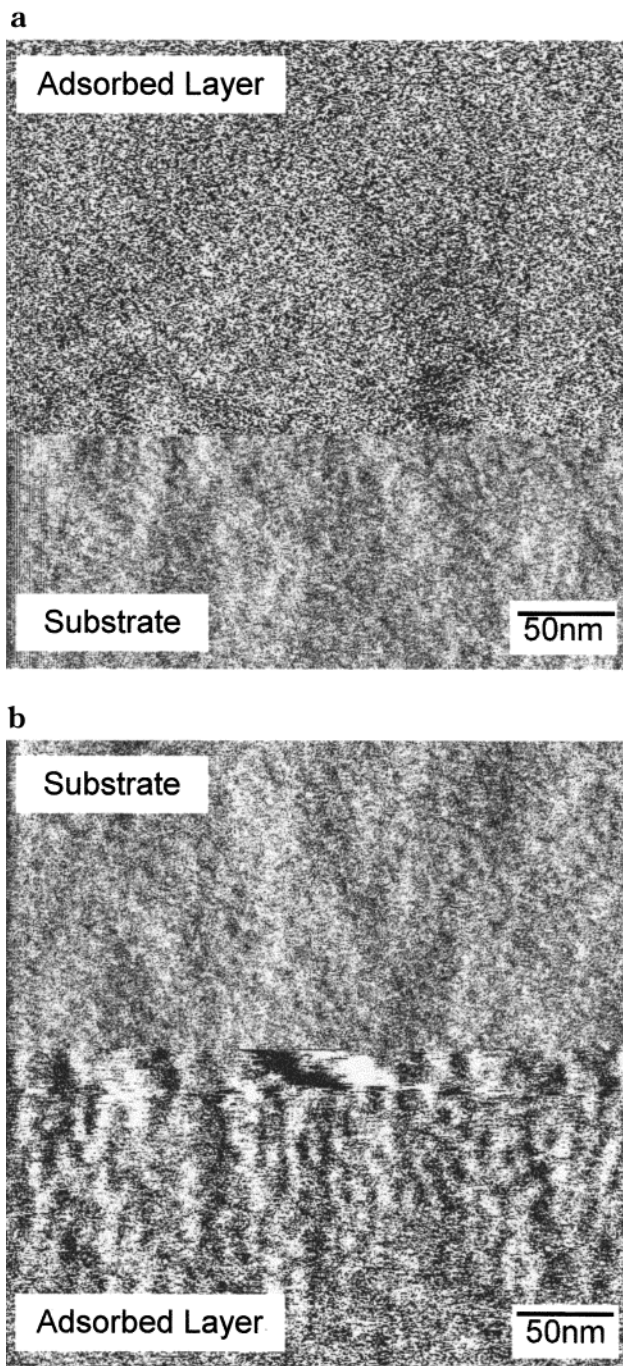


Figure 7. (a) AFM image obtained of the silica–solution interface after immersion in an aqueous solution of 0.30 mM CPBr for 20 min. No discernible structures are visible. The slow scan direction is down the page. The underlying silica surface is imaged in the lower portion of the page when a higher imaging force is applied. (b) AFM image obtained of the silica–solution interface after immersion in an aqueous solution of 0.30 mM CPBr for 22.5 h. Evidence of some structural order in the surfactant layer is observed. The slow scan direction is up the page. The underlying silica surface is imaged in the upper portion of the page when a higher imaging force is applied.

charge neutral. Thus, only weak double-layer interactions would be expected, and the interaction should be dominated by the dispersion forces, as is seen. In the presence of 0.3 mM CPBr, the force data exhibit a long-range repulsive interaction that decays exponentially with distance, as is expected for an electrical double-layer interaction, indicating that both surfaces now carry a significant charge of the same sign. These data offer strong

(30) Senden, T. J.; Drummond, C. J.; Kekicheff, P. *Langmuir* **1994**, *10*, 358–362.

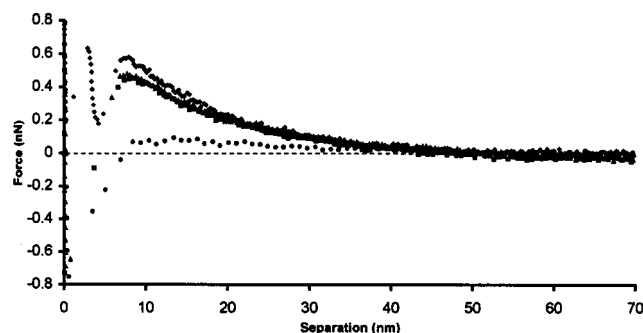


Figure 8. Force vs apparent separation for the interaction of an AFM cantilever probe (Digital Instruments, Si_3N_4 , contact-mode cantilever $k \sim 0.21 \text{ N m}^{-1}$) with a flat silica substrate immersed in an aqueous solution of 0.3 mM CPBr. The data were collected at 10 min (triangles), 270 min (squares), and 20.5 h (diamonds) after injection of the surfactant solution. Data are also shown for the same system in pure water (circles). All data were collected at a pH of 5.5 ± 0.3 and at a constant temperature of $25 \pm 0.1 \text{ }^\circ\text{C}$.

evidence that sufficient CPBr is adsorbed within 10 min to result in a charge reversal of the silica surface. Data collected between 10 and 270 min of immersion in 0.30 mM CPBr display a jump into contact from $\sim 8 \text{ nm}$ as the gradient of the force exceeds the spring constant. This distance is too large to be attributed to penetration of the tip through an adsorbed surfactant layer or simple van der Waals forces. This jump is therefore thought to be due to a hydrophobic attraction between exposed monomer tail groups in the partially formed surfactant layers. After 20.5 h, the data again show a long-range electrostatic component. However, now at small separation distances a steeply repulsive region is also seen, beginning at a separation of about 5 nm. A final push through jump-to-contact is then seen at 4-nm separation. These data are typical of adsorbed surfactant structures at the solid–liquid interface.⁵

We will first address the origin of the SAR and second address what determines the boundaries of the SAR. It would appear that surface-adsorbed aggregates are the thermodynamically stable arrangement of adsorbed surfactant at 0.3 mM CPBr. However, the slow rate of adsorption indicates that there are kinetic barriers to the formation of these structures. As these concentrations are below the solution CMC, adsorption should only be due to monomers. These monomers must participate in an aggregation process at the surface that results in the formation of surface structures analogous to bulk micelles. During this process, a monomer may have to sample many sites before it is successfully incorporated into a surface aggregate. Additionally, an incoming monomer must also overcome an electrostatic barrier to reach the surface, as the surface excess of 0.4 mg m^{-2} is sufficient to cause charge reversal of the silica surface. Thus, we conclude that the SAR is a result of kinetic barriers to the adsorption process in the form of structural and electrostatic components.

The boundaries of the SAR are determined both by the surface structure and coverage and by the aggregate structure of surfactant in solution. At concentrations below the SAR, the concentration in bulk is not sufficient to raise the chemical potential of the monomer to a level where surface aggregation is favorable. The surface excess therefore indefinitely remains below that required to give rise to surface aggregates. At concentrations above the SAR, surface aggregates are clearly forming and are doing so rapidly. One explanation is that at concentrations above

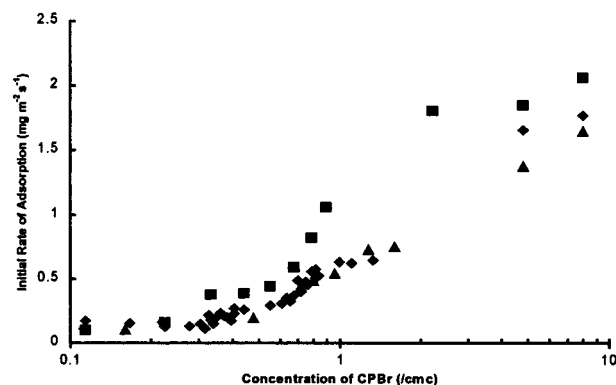


Figure 9. Initial rates of surfactant adsorption to the silica–solution interface vs solution CPBr concentration in the presence of 0.01 M KBr on pyrogenic silica (triangles) and in the absence of 0.01 M KBr on pyrogenic (squares) and hydroxylated (diamonds) silica. The concentration of CPBr has been normalized by the corresponding CMC (0.75 mM without electrolyte and 0.1 mM in the presence of 0.01 M electrolyte).

the SAR but below the CMC a number of transient semiformed aggregates are present in solution and these premature aggregates adsorb to the surface, negating any requirement for monomer units to slowly pack into a preformed aggregate structure. Supporting this is our observation that the normalized adsorption or sticking ratio (explained below) above the CMC is higher than the sticking ratio below the CMC. This indicates that a monomer in an aggregate has a greater chance of adsorbing to the surface than a free monomer. Alternatively, as the bulk surfactant concentration is increased, the electrostatic repulsion between the monomer and the surface will be screened more effectively. This will decrease the energy barrier to adsorption for monomers and facilitate more rapid accumulation at the surface.

The SAR has not been observed in the presence of electrolyte. Added electrolyte will both screen the double layer and lead to a greater polydispersity in bulk micelles. It is thought that, as the addition of electrolyte lowers the electrostatic repulsion of the double layer and the head-group area, the electrostatic and steric barriers to the incorporation of surfactant monomers into adsorbed structures are reduced. Additionally, the CMC will also be more obtuse, and below the accepted CMC, some transient semiformed micelles may still be present. These micelles may have a role in adsorption at the surface and negate the need for monomeric surfactants to pack into a surface aggregate.

Rapid Adsorption Region. While an optical reflectometer is useful for determining the equilibrium surface excess, it is particularly suitable for studying the fast kinetics associated with adsorption that cannot be elucidated using traditional techniques. The initial rate of adsorption is simply determined from the measured change in surface excess with time, immediately following the introduction of the surfactant solution into the experimental cell. This gradient is found to be initially linear. The initial rates of adsorption for CPBr on pyrogenic and hydroxylated silica and CPBr in 10 mM KBr on pyrogenic silica are presented in Figure 9. Here, the surfactant concentration has been normalized by the CMC to aid the comparison. The rate of adsorption increases with concentration below the CMC, and a discontinuity appears in the data at the CMC. Importantly, the rate of adsorption continues to increase with concentration above the CMC. This indicates that micelles have a definite role in the initial adsorption process.

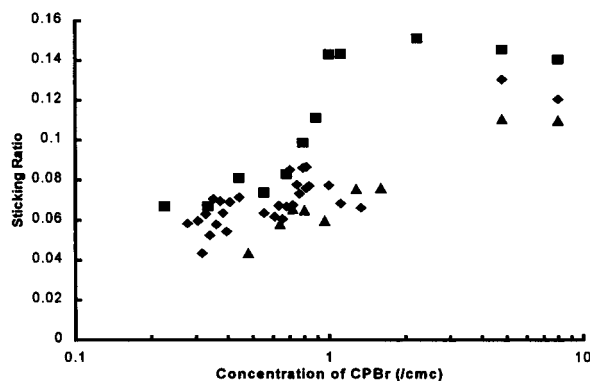


Figure 10. Sticking ratio (determined from the initial rate of adsorption) vs CPBr concentration in the presence of 0.01 M KBr on pyrogenic silica (triangles) and in the absence of 0.01 M KBr on pyrogenic (squares) and hydroxylated (diamonds) silica. The concentration of CPBr has been normalized by the corresponding CMC. The theoretical DLF to the surface (J) is calculated from $J = 0.776\nu^{1/3}R^{-1}D^{2/3}(\alpha Re)^{1/3}c$, where the values of the variables used in the calculation of the theoretical DLF were as follows: mean fluid velocity (u) = 0.0022 m s⁻¹, radius of inlet tube (R) = 0.0013 m, kinematic viscosity (ν) = 8.93 × 10⁻⁷ m² s⁻¹, Reynolds number (Re) = 3.37, radius of gyration (a) = 2 × 10⁻⁹ m, diffusion coefficient (D (monomer)) = 1.21 × 10⁻¹⁰ m² s⁻¹, D (micelle) = 8.36 × 10⁻¹¹ m² s⁻¹, distance between inlet tube and surface (h) = 0.0015 m, dimensionless flow intensity parameter α = 6, and the concentration (c) in kilograms/meters cubed of the surfactant solution. The sticking ratio increases at the CMC for both systems.

The use of an optical reflectometer with a stagnant point flow cell geometry and the well-defined hydrodynamic flow fields associated with it permits the measured rate of adsorption to be compared to the theoretically derived diffusion-limited flux (DLF) to the surface.³¹ The quotient of these two values is recorded as the sticking ratio²⁰ and is simply the amount of surfactant molecules that are adsorbed to the surface normalized by the theoretically derived DLF to the surface. Note that this is an oversimplification of the actual process, as adsorbed surfactant molecules are freely exchanging with surfactant in the bulk. An increase in sticking ratio with concentration indicates cooperativity, while a constant sticking ratio suggests that surfactant molecules are adsorbing independently. However, trends in sticking ratio can give valuable insight into the nature of the adsorption process. The sticking ratios for CPBr on hydroxylated and pyrogenic silica are presented in Figure 10, with the concentration normalized by the CMC. Above the CMC, the theoretical flux is determined as the sum of the flux due to micelles and the flux due to monomers, and any concentration increase above the CMC is reflected only in the flux due to micelles, as the monomer concentration is assumed to be static. The important result from this figure is the marked increase in the sticking ratio for all systems at the CMC, indicating an increase in the efficiency of the adsorption process above the CMC. If surfactant molecules were competing for adsorption sites, this would be reflected in a reduction in the sticking ratio. Below the CMC, the sticking ratio is gradually increasing. This increase is most likely due to the presence of some aggregates below the CMC. The sticking ratio increases sharply at the CMC for the pyrogenic, hydroxylated, and electrolyte systems, respectively, which clearly indicates that above the CMC adsorption has become cooperative.

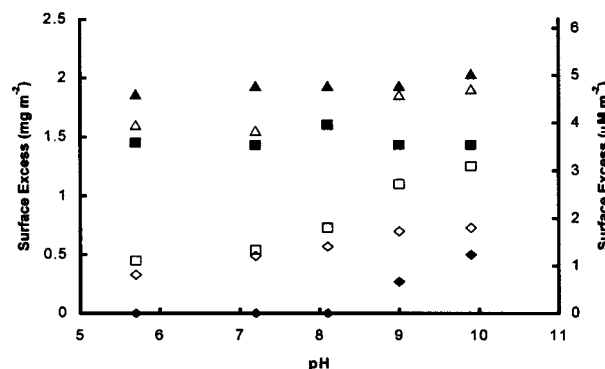


Figure 11. Measured surface excess vs pH for 1.08 mM (surfactant concentration 3, C3) CPBr with no electrolyte (open triangles) and with 0.01 M KBr (filled triangles); 0.09 mM (C2) CPBr with no electrolyte (open squares) and with 0.01 M KBr (filled squares); and 0.0042 mM (C1) CPBr with no electrolyte (open diamonds) and with 0.01 M KBr (filled diamonds).

The most obvious explanation for cooperativity is that micelles are directly adsorbing to the surface, either partly or wholly. For this to lead to the observed trend in sticking ratio, the increased success with which micelle-bound monomers adsorb to the substrate must be due to more effective penetration of the electrical double layer by micelles as compared to monomers. Opposing adsorption is the electrostatic repulsion of the double layer, and as a micelle has a significant number of counterions associated with it, we propose that surfactant contained within a micelle will more effectively penetrate the double layer than a monomer. This is due to the reduced charge per monomer contained in a micelle.

Adsorption and pH. Figure 11 shows the relationship between the pH and the surface excess for three CPBr concentrations with and without added electrolyte. Increasing the solution pH has two important effects. First, the electrophoretic mobility of silica particles rises as the pH of the bulk solution is increased.³² This is due to the ionization of the surface hydroxyl groups, which increases the negative charge of the surface and hence the particle mobility in an electric field. Thus, the silica surface charge will increase with pH.³² Second, the solution ionic strength increases with pH in a logarithmic fashion. An increase in ionic strength screens the interaction between charges and thereby reduces the surfactant headgroup area. This second effect will only be important in the absence of added electrolyte, as when 0.01 M KBr is present the ionic strength increase imparted by adjustment of the pH is negligible. Three surfactant concentrations were chosen where C1 < C2 < C3. Concentration C1 (0.0042 mM) is below that required for charge reversal of the silica substrate. Concentration C2 (0.09 mM) is above that required to neutralize the surface charge but below the solution CMC, and concentration C3 (1.08 mM) is above the solution CMC. These statements are true for both the electrolyte and the no-electrolyte systems.

At concentration C1, the surface excess increases with increasing pH and is always greater in the absence of electrolyte. The electrolyte is therefore inhibiting the adsorption of surfactant. What is the nature of this competition? At pH 5.5, the surface excess is very low and insufficient to neutralize the surface charge; therefore, adsorption is completely electrostatically driven. Surfactant monomers are competing with the cations of the electrolyte for adsorption sites. As the pH is increased,

(31) Dabros, T.; van de Ven, T. G. M. *Colloid Polym. Sci.* **1983**, *261*, 694.

(32) Hunter, R. J. *Foundations of Colloid Science*; Oxford University Press: New York, 1985.

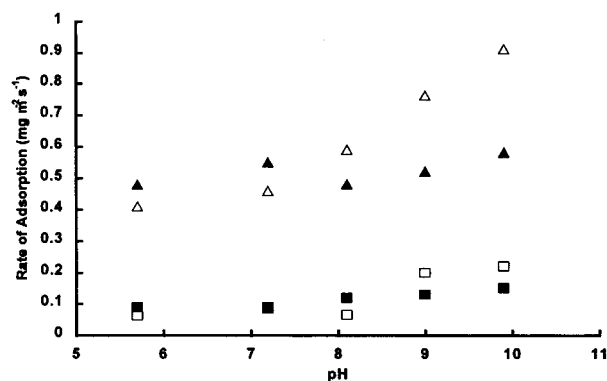


Figure 12. Measured initial rate of adsorption vs pH for 1.08 mM (surfactant concentration, C3) CPBr with no electrolyte (open triangles) and with 0.01 M KBr (filled triangles) and 0.09 mM (C2) CPBr with no electrolyte (open squares) and with 0.01 M KBr (filled squares).

the surface charge increases, resulting in an increase in surfactant adsorption. Additionally, in the absence of background electrolyte, the headgroup area decreases, favoring lateral hydrophobic interactions and cooperative adsorption. This results in an increase in surface excess and a reversal of surface charge. In the presence of electrolyte, there is no detectable adsorption below pH 8.0. Above pH 8.0, the number of charged sites on the surface rises sufficiently to bring about increased and measurable surfactant adsorption. The surface excess is now sufficient to bring about lateral hydrophobic interactions and charge reversal. However, the surface excess remains below that achieved in the absence of electrolyte due to the competition between the cations of the electrolyte and the monomers for charged surface sites. In the presence of electrolyte, the headgroup area will be smaller, and this favors cooperativity, but the unfavorable competition for surface sites dominates, ensuring that the surface excess is lower in the presence of electrolyte.

At concentrations C2 and C3, the surface excess has increased and is always greater in the presence of electrolyte, unlike at concentration C1. Clearly, the screening of the headgroup charge by electrolyte, which favors hydrophobic interactions, is dominating the adsorption behavior. In the presence of electrolyte, the surface excess is unchanged upon increasing the pH, while in the absence of electrolyte the surface excess steadily increases with pH. This can be attributed to the increased ionic strength associated with increasing the pH. The surface excess in the two systems is most similar at pH 10, where the ionic strength of the no-electrolyte system is closest to the electrolyte system.

The kinetics of adsorption reveal complex adsorption behavior as a function of pH, as shown in Figure 12. Only the two higher concentrations are shown as the low surface excesses for the other concentration lead to large uncertainties in the calculated rate of adsorption. With a background electrolyte of 10 mM KBr, the rate of adsorption is not affected significantly by increasing solution pH. However, in the absence of electrolyte, the rate of adsorption increases markedly between pH 7.0 and pH 10.0, exceeding the rate observed in the presence of electrolyte.

The ionic strength will affect the rate of adsorption in two ways. First, an increase in ionic strength will result in greater screening of charge between adsorbed monomers and incoming monomers, thereby increasing the rate of adsorption (note that the technique is only sensitive to the kinetics of adsorption at surface excesses greater than

that required for charge reversal). This effect will be most marked at low electrolyte concentrations, where a small increase in electrolyte concentration results in a large increase in the screening length. Second, an increase in ionic strength will provide more cations to compete with monomers for charged surface sites and thereby decrease the rate of adsorption. The electrolyte concentration will determine which of these two effects dominates. In the presence of electrolyte, the initial rate of adsorption remains unchanged with increasing pH. This indicates that the surface charge is not determining the adsorption rate. In the absence of electrolyte, a significant increase in the initial rate of adsorption with increasing pH is observed. This increase is attributable to greater screening of charge between adsorbed monomers and incoming monomers. Below pH 7.0, the adsorption rate in the presence of electrolyte is higher than that obtained without electrolyte. Above pH 7.0, the reverse is true. Why then is the adsorption rate above pH 7.0 in the presence of electrolyte lower? The much greater number of cations in the electrolyte system must be slowing surfactant adsorption by competing for surface charge sites. Therefore, there must exist intermediate electrolyte levels where the rate of adsorption is a maximum over the surfactant concentration range of C2 to C3. This will occur at low electrolyte concentrations, the headgroup charge will be poorly screened, but there will be little competition from cations for surface sites. At the concentration of maximum adsorption rate, the headgroup charge will be screened, but monomers will still readily access surface charge sites. As the electrolyte concentration is increased further, the rate of adsorption will decrease as cations prevent some monomers from accessing surface charge sites. The further increase in screening must not be sufficient to compensate for this.

Conclusion

Optical reflectometry and AFM have been used to investigate the adsorption of CPBr to the silica–water interface as a function of CPBr concentration, with and without added electrolyte, and as a function of pH. AFM imaging and reflectometry adsorption studies reveal that, in the absence of electrolyte, admicelles (called lucano after their shape) are present on the silica surface. The lucano cover ~45% of the surface, are typically ~2 nm thick and ~8.4 nm in diameter, and are approximately cylindrical in shape with the circular surfaces being parallel to the silica substrate. When electrolyte is present, the surface structures become elongated in the plane of the surface. Adsorption kinetics were also studied in detail. The bounds of the SAR were determined. The SAR is thought to arise from structural rearrangements in the adsorbed surfactant layer. The evolution of these structures was followed by AFM. No SAR region was found in the presence of 0.01 M KBr. Adsorption as a function of pH revealed complex behavior. The effect of pH on the equilibrium surface excess and the rate of adsorption is determined by competition between electrolyte cations and surfactant monomers for silica binding sites and screening of charge–charge interactions by the electrolyte.

Acknowledgment. The authors thank G. Spinks of the University of Wollongong for generously providing access to an ellipsometer, B. D. Fleming for kind assistance with AFM imaging, S. M. Notley for assistance with the collection of force curves, and E. J. Wanless for her review of the manuscript.